

## Combustion Synthesis of $\text{LiMn}_2\text{O}_4$ with Citric Acid and the Effect of Post-heat Treatment

Yi-Sup Han<sup>†</sup>, Jong-Tea Son\*, Ho-Gi Kim and Hun-Teak Jung\*\*

Dept. of Mat. Sci. & Eng., Korea Advanced Institute of Science and Technology (KAIST), Teajon 305-701, Korea

\*Dong-A Electric Equipment Co. LTD., Seoul 132-042, Korea

\*\*Department of Ceramic Engineering, Dongshin Univ. Naju, Chonnam 520-714, Korea

(Received December 3, 2000, Accepted March 5, 2001)

### ABSTRACTS

Combustion process with citrate was used to produce the  $\text{LiMn}_2\text{O}_4$  powder. Precursors are pre-ignited in open air followed by post-heating in the range from 600 °C to 800 °C for 4 h. With varying the molar ratio (R) of ethylene glycol (EG) to citric acid (CA) from 0 to 4, the effect of EG content on powder characteristics is evaluated. Vacuum drying promote the auto-ignition at room temperature. With small addition of EG metal ion was selectively segregated with organic substances and undesired lithium evaporation occurred during post-heating.  $\text{LiMn}_2\text{O}_4$  phase which is produced by combustion reaction was decomposed back to  $\text{Mn}_3\text{O}_4$  because the reaction temperature was higher than 950 °C. With increasing EG content, the homogeneity of  $\text{LiMn}_2\text{O}_4$  powder increased and specific surface area increased. And lithium evaporation during vacuum drying and/or ignition also increased.

**Key words :** Combustion synthesis,  $\text{LiMn}_2\text{O}_4$ , Citric acid, Post-heat treatment, Vacuum drying

### 1. Introduction

Lithium Manganese spinel is a candidate electrode material for lithium ion batteries<sup>1)</sup> because manganese oxides offer advantages in terms of specific energy, toxicity and costs.<sup>2)</sup> The capacity loss of the lithium spinel during cycling has become an area of interest to both electrochemists and ceramists. Several attempts have been made to solve this problem by wet chemical method, such as, emulsion drying method,<sup>3,4)</sup> precipitation method<sup>5)</sup> and sol-gel method.<sup>6,7)</sup> Among them Pechini process<sup>7)</sup> can produce a capacity above 130  $\text{mAhg}^{-1}$  together with excellent cycling behaviour. Experimentally, the volume of the powder abruptly expanded during calcination in Pechini process,<sup>8)</sup> because auto-ignition is initiated in the furnace.

In this work, the Pechini process, to produce the  $\text{LiMn}_2\text{O}_4$  powder, has been modified such that the precursors are pre-ignited in open space before calcination in order to prevent contaminating the furnace and to supply sufficient oxygen to the sample. The powder characteristics are evaluated with varying the amounts of EG

### 2. Experimental Procedure

Schematic diagrams of this process is given in Fig. 1. Metal nitrate solution is prepared as followings because the manganese nitrate and lithium nitrate are very hygroscopic. Reagents of  $\text{MnO}_2$  (Aldrich Chemicals; 99%) was dissolved in 2M-nitric acid (dilution of 60%  $\text{HNO}_3$ ; Oriental

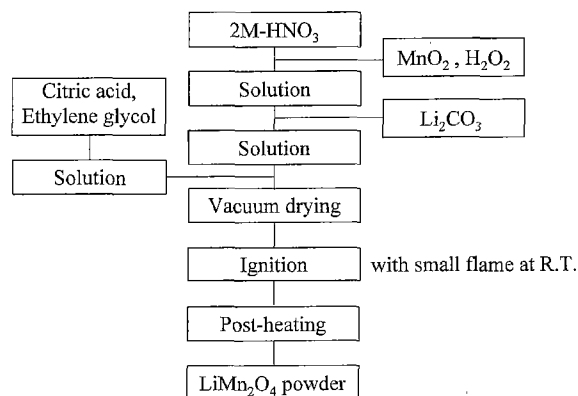


Fig. 1. Flow chart for the preparation of  $\text{LiMn}_2\text{O}_4$  powders.

Chemicals) with several drops of hydrogen peroxide (Junsei Chemicals; 30%) until a clear solution was obtained.<sup>9)</sup> Stoichiometric amounts of  $\text{LiCO}_3$  were then dissolved to this solutions.

Pre-dissolved solutions of CA (Aldrich Chemicals; 99.5%) and EG (Junsei Chemicals; extra pure) with a molar ratio (R) of EG to CA 0, 1, 2 and 4 were added to the clear metal nitrate solutions. The mixed solutions were stirred on hot plate, which allowed the temperature to be controlled below about 200 °C because abrupt heating leads to combustion reaction at the bottom of the beaker,<sup>10)</sup> until the solutions become dark brown gel. This was followed by drying in vacuum to evaporate the residual water at 120 °C. The temperature of the vacuum dryer is raised by steps of 20 °C when the liquid condensed on the window of the vacuum dryer is com-

<sup>†</sup>Corresponding author : yshan@netian.com

pletely dried, At 180°C, the last stage of drying, a sample was left in dryer for overnight to obtain completely dried precursor. The puffed precursors were transferred to stainless steel tray and auto-ignition was initiated by the flame of a gas lighter. The ash converts into more expanded form. The ignited powders were post-heat treated at 600°C, 700°C and 800°C for 4h in air with heating rate of 3°C/min. The cooling rate was 0.5°C/min. and 3°C/min. to 500°C and room temperature, respectively.

The thermal decomposition behavior of the dried precursors before ignition was examined by means of thermogravimetry (TG) and differential scanning calorimeter (DSC) at a heating rate of 5°C/min. in air with STA409 instrument from Netzsch. Phase analysis was carried out by powder X-ray diffraction (XRD) with Cu K $\alpha$  radiation in a Rigaku X-ray diffractometer. Scanning electron micrographs (SEM) were obtained to examine the morphology of the powder. The specific surface area was measured by the Brunauer-Emmett-Teller (BET) method using N<sub>2</sub> gas. Induction coupled plasma (ICP) was used to determine the lithium contents of the sample.

### 3. Results and Discussion

Apparent variations of solutions during drying and ignition actions are shown in Table 1. The colors of solution have changed from light pink to yellow by adding the chelating polymers and heating. During evaporating the water from the mixed solution, precipitates of polymer, which have light-brown color, were observed in the samples of small addition of EG (in Table 1. R0, R1, R0-Mn).

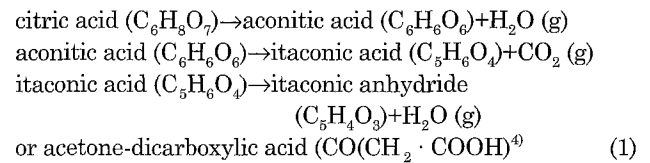
With no addition of EG (R0, R0-Mn), the esterification and polymerization reactions<sup>7,8)</sup> did not occur, because of the absence of the hydroxyl groups of EG. A solid with a brown-color was obtained instead of polymeric gel. In this case, there is no necessity for vacuum drying for the completion of drying. With the addition of one mol of EG, a little precipitation occurred at the intermediate stage of drying, but finally dark brown gel was obtained.

The vacuum dried precursors (R1, R2 and R4) took the form of a sponge-like black solid (char) because of the evaporation of gaseous product from the esterification reaction. The apparent volume of precursor was greater for an addi-

tion of 4 mol of EG and, therefore, it means that this is the optimal gelling condition.<sup>7)</sup> A flame of the cigarette lighter could initiate auto-ignition of this char at room temperature in air. The ignited precursor, the ash, expanded again during combustion reaction. Ignition was completed within 10 min.

The precursors of R0-Mn treated in vacuum dryer is also auto-ignited at room temperature, while the sample R0 had to be subjected to additional heating on hot plate for ignition. Therefore, it is clear that the initiation of the ignition at room temperature needs vacuum drying.

The thermal decomposition behaviors of vacuum dried precursors from solutions with R0-Mn, R1 and R4, compared with the as-received-CA are presented in Fig. 2. In case of citric acid (Fig. 2 (d)), there are two endothermic peaks, which are not shown in the precursors (R0-Mn, R1, R4). The one is melting (158.1°C) of the citric acid, the other is related to the decomposition reaction as equation (1).<sup>7)</sup>



The Endothermic peaks at 103°C in R1 and R4 (Fig. 2 (b) and (c)) represent the evaporation of residual water which is probably produced by the polymerization reaction. The exothermic peaks in the range of 200°C~360°C, resulting from the modification of the molecular structure during vacuum drying, can make the initiation of the ignition at room temperature with small frame and then leading to self propagation of combustion reaction.

With increasing EG, exothermic peaks at higher temperature have higher intensity. Decomposition reaction in all samples complete below 360°C. It means that all the organic substances in the precursors are burned out below this temperature. In R0-Mn (Fig. 2 (a)), a broad endothermic peak near 450°C, which is accompanied with weight loss, is probably a oxidation reaction of the residual carbon or reduction of Mn<sub>2</sub>O<sub>3</sub> to Mn<sub>3</sub>O<sub>4</sub>.<sup>11)</sup>

The morphology of ignited powders are given in Fig. 3. It is found that the primary particle size of all conditions have

Table 1. Apparent Variations of Precursor Solution with CA and EG during Drying and Igniting Action

Sample No.	Metal content	EG content (R)	Drying stage			Vacuum drying treatment	Auto-ignition at room temperature
			Initial	Intermediate	Final		
R0	1Li+2Mn	0	Light pink	Yellow, ppt	Solid	No treating	No reaction
R1	1Li+2Mn	1	Light pink	Yellow, ppt	Gel	Treating	Reaction
R2	1Li+2Mn	2	Light pink	Yellow	Gel	Treating	Reaction
R4	1Li+2Mn	4	Light pink	Yellow	Gel	Treating	Reaction
R0-Mn	Mn only	0	Light pink	Yellow, ppt	Solid	Treating	Reaction

Citric acid content was equal to total metal ion content in mol.

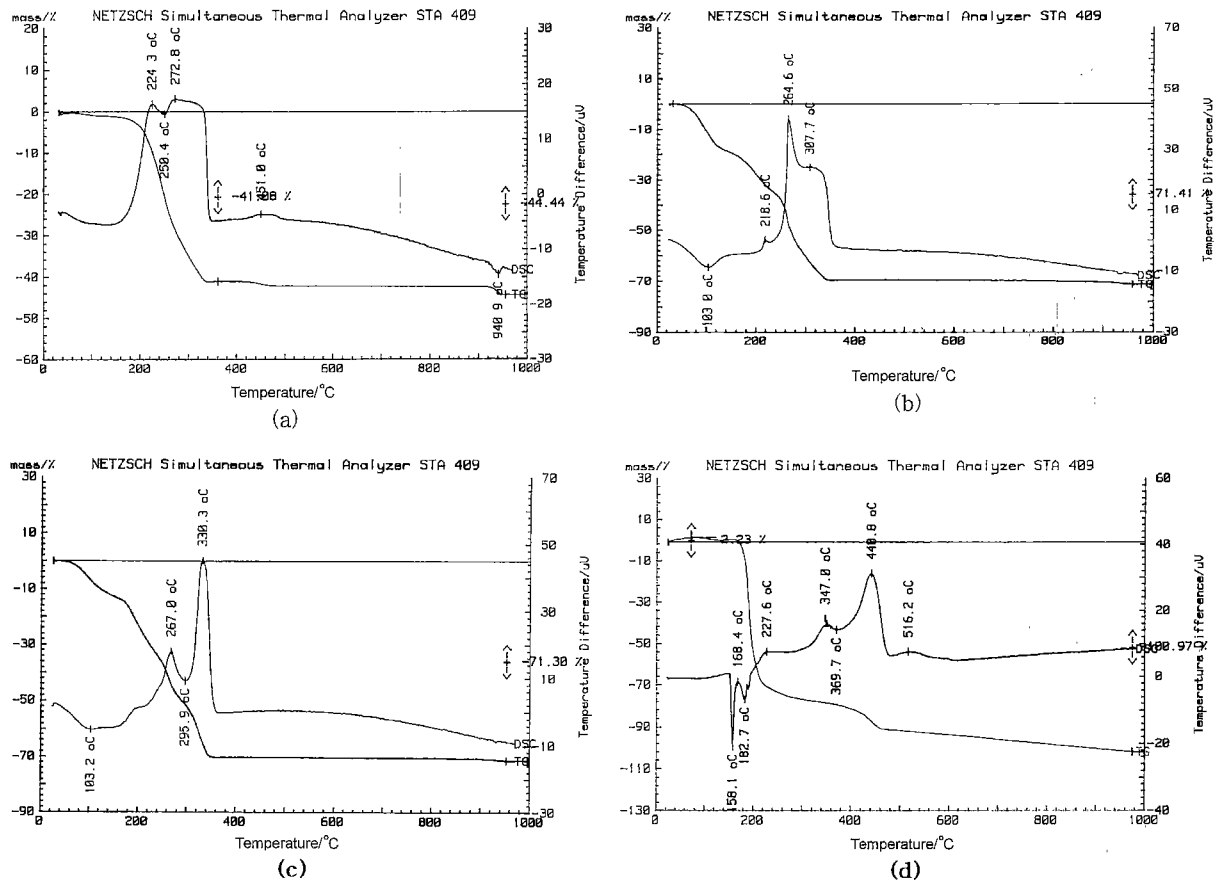
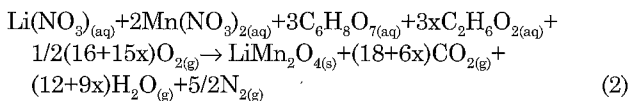


**Fig. 2.** TG/DSC curves of precursors after vacuum drying from solutions with (a) R0-Mn, (b) R1 and (c) R4, compared with (d) the as-received-C.A.

the order of  $\sim 0.1 \mu\text{m}$ , and there are many pores of which the size is 10 times the primary particle. The particle shape is different from each other. In case of R0, there are many primary particle between the pores (in marking of circle). But in the other cases (R1, R4), mono layer of the primary particle spread to form a flake-like particle.

It can be explained in terms of the 'Fuel-Oxidizer Concept' proposed by Jain *et al.*<sup>12)</sup> vis.,  $\text{NO}_3$  of nitric acid can act as an oxidant and polymers (CA and EG) as a fuel. Therefore, the following reaction can be assumed for the combustion reaction of precursors.



Where x is equal to the ratio of R.

As the more EG was added, the more gas evaporated during reaction, therefore, there are more pore within the particle. Consequently, resulting morphology of the particles has a lot of pore with increasing EG.

The XRD patterns of the ignited powder is given in Fig. 4. It is found that the  $\text{LiMn}_2\text{O}_4$  phase could crystallize within a few minutes during ignition. The  $\text{Mn}_3\text{O}_4$  phase is also detected. From Mn-O phase stability diagram (Fig. 5), we

can see that the  $\text{Mn}_3\text{O}_4$  phase is stable above about  $950^\circ\text{C}$  in air. If the reaction temperature was lower than  $950^\circ\text{C}$ , the oxygen partial pressure in ignition reaction should be very low in spite of the open air. From eq. (2), theoretical oxygen amount of all the experimental condition can be calculated and the results are plotted in Fig. 6. It is clear that if more EG was added, more oxygen is required to burn out all the chelating polymers. But the reaction speed is slow enough to supply the oxygen from air, therefore, the partial pressure of oxygen near the particle surface might be close to ambient condition.

Aruna, *et al.*<sup>13)</sup> have reported that the temperature of the flame during auto-ignition is  $900 \pm 50^\circ\text{C}$ . The lightness of the combustion flame of all the precursors was as bright as that of the frame of the charcoal. Therefore the temperature of combustion flame of the precursor is thought to be higher than  $950^\circ\text{C}$ . At this temperature,  $\text{LiMn}_2\text{O}_4$  phase which is produced by combustion reaction, can partly be decomposed back to  $\text{Li}_2\text{O}$  and  $\text{Mn}_3\text{O}_4$ .

$\text{Mn}_3\text{O}_4$  peaks of R0 sample is sharper and higher than that of the others (Fig. 4 (a)). It is concluded that the precipitation during drying the solution should be selective segregation of Li and Mn (non-homogeneous gel), respectively.

Because the samples in all the conditions have low crystallinity (Fig. 4) and contain impurity phase ( $\text{Mn}_3\text{O}_4$ ) which

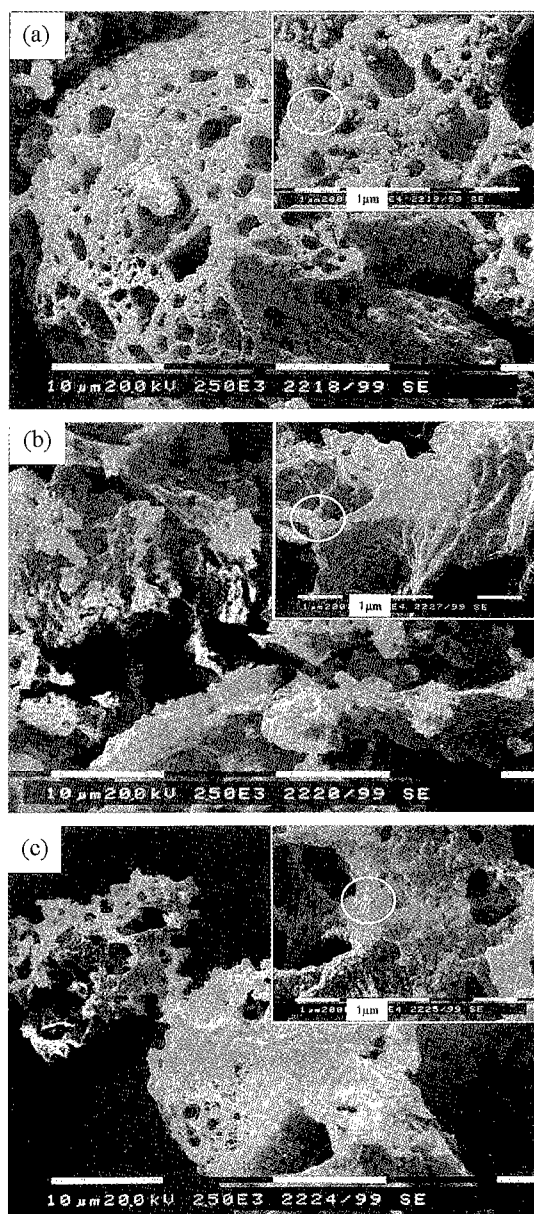


Fig. 3. Scanning electron micrographs of ignited powders with different EG content, where inset shows the enlarged view. (a) R0, (b) R1 and (c) R4.

is electrochemically inactive, post-heat treatments are needed for lithium secondary battery.

The lithium contents of synthesized powders before and after post-heat treatment at 800 °C for 4h with each EG contents are given in Fig. 7. Lithium contents is decreased with EG contents in as-ignited powder (before post-heat treatment). Many gaseous substances (EG (b.p. ; 196-198 °C) and reaction product of eq. (1)) are produced during vacuum drying. Therefore, lithium ion combined with this substances could be easily evaporated. Moreover, if the excessive EG is added, larger amounts of gaseous products and more exothermic heat of the decomposition reaction could promote the evaporation of lithium during ignition.

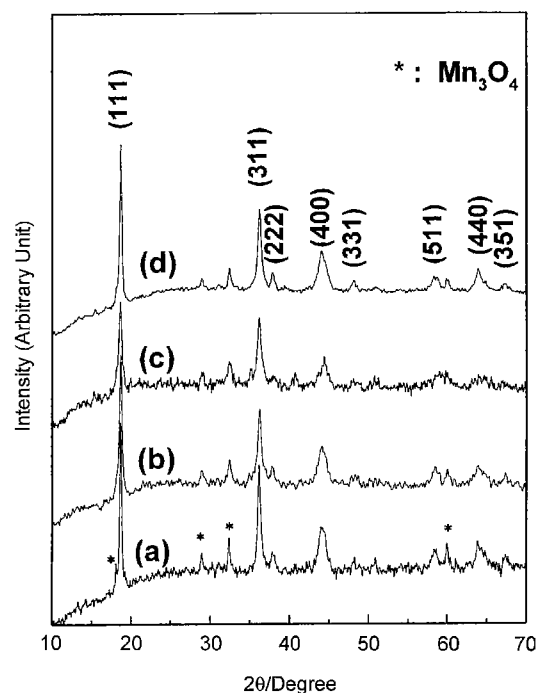


Fig. 4. XRD patterns of ignited precursors with different EG addition: (a) R0; (b) R1; (c) R2; (d) R4.

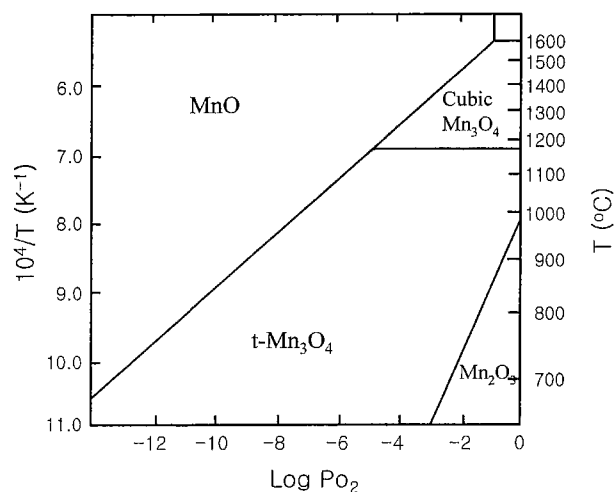


Fig. 5. Mn-O phase stability diagram.

The XRD patterns of powders after post-treatment are presented in Fig. 8. When no EG (Fig. 8 (a), R0) is added to the solution, a large amount of  $Mn_2O_3$  is detected and the lowest lithium contents is obtained (Fig. 7). It is concluded that lithium is evaporated again in sample with low EG content during post heat treating.

The final morphology of the heat treated powder are given in Fig. 9. With a small addition of EG (R=0, 1), there are abnormally coarsened particles (marked by arrows in (a) and (b)).

In previous<sup>14)</sup> report, there are two step reactions on the chemistry of the  $LiMn_2O_4$  formation from  $Li_2O$  and  $Mn_2O_3$ .

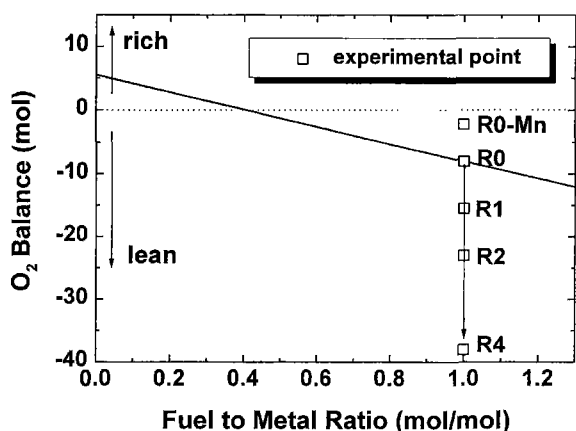


Fig. 6. The experimental points on the oxygen balance vs fuel/metal ratio diagram.

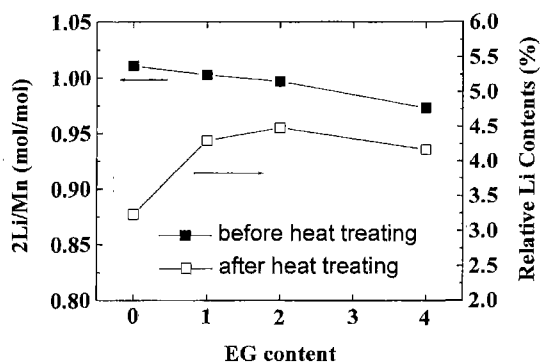
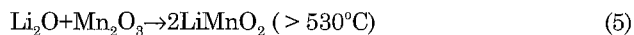
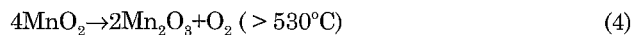
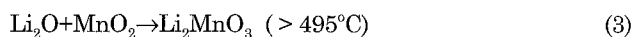
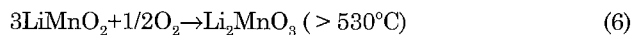


Fig. 7. Lithium contents of (a) ignited powders and (b) post-heat treated powders at 800°C for 4 h with respect to EG content.

In the first main step, the following three reactions are proceeded.



The products of this three intermediate reaction ( $\text{Li}_2\text{MnO}_3$ ,  $\text{Mn}_2\text{O}_3$  and  $\text{LiMnO}_2$ ) are electro-chemically inactive in the 4V range versus  $\text{Li}/\text{Li}^+$ . The second main step is as follows.



It is evident that reaction (6) cannot proceed if, for example, the orthorhombic phase  $\text{LiMnO}_2$  is covered by preliminary nucleated spinel  $\text{LiMn}_2\text{O}_4$  and by rock-salt phase  $\text{Li}_2\text{MnO}_3$  whereby the access of  $\text{O}_2$  to the orthorhombic phase will be strongly hindered. Similarly, reaction (7) cannot proceed if the rock-salt phase  $\text{Li}_2\text{MnO}_3$  is separated from

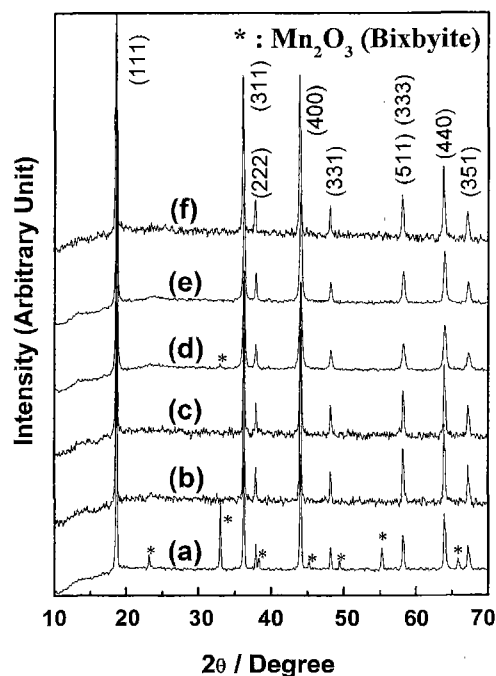


Fig. 8. XRD patterns of  $\text{LiMn}_2\text{O}_4$  powders post-heated at 800°C for 4 h with various EG content: (a) R0; (b) R1; (c) R2; and post-heated at (d) 600°C, (e) 700°C and (f) 800°C for 4 h from R4 sample.

the  $\text{Mn}_2\text{O}_3$  grain by  $\text{LiMn}_2\text{O}_4$  preliminary nucleated between them, because the two phases ( $\text{Li}_2\text{MnO}_3$  and  $\text{Mn}_2\text{O}_3$ ) are thermodynamically stable in the 500-750°C temperature range, usually applied for the preparation of the  $\text{LiMn}_2\text{O}_4$  spinel. Obviously the last two reactions (6) and (7) have the tendency to autoblock themselves, and this can be a source of considerable impurities in the final product.

As mentioned above, the drying of solutions for R0 and R1 produces precipitates. Therefore the following conclusions are drawn. For R=0, the lumps of Li-rich and Mn-rich phases segregated out (inhomogeneous gel) during drying the solution. The previous hindering effects of reactions (6) and/or (7) could easily happen during the post heating of inhomogeneous powder because it is also solid state reaction. Therefore residual lithium in Li-rich phase were evaporated during heating. Moreover,  $\text{Mn}_2\text{O}_3$  has a considerably greater tendency of crystal growth by solid-state reaction than  $\text{LiMn}_2\text{O}_4$ .<sup>15)</sup> This will promote lithium evaporation. Consequently, by increasing EG, the homogeneity of metal cation could depress lithium evaporation during post heating, while specific surface area increased (Fig. 10). A trace of  $\text{Mn}_2\text{O}_3$  is also detected in the powder which is ignited with R4, followed by heat treating at 600°C for 4hr (Fig. 8 (d)), and further heating resulted in a single phase spinel (Fig. 8 (e) and (f)).

The dependance of the lattice parameter of the  $\text{LiMn}_2\text{O}_4$  upon EG content and post-heating temperature is shown in Fig. 11. Both the molar ratio of the EG to CA and post-heating temperature influence the lattice parameter. The lat-

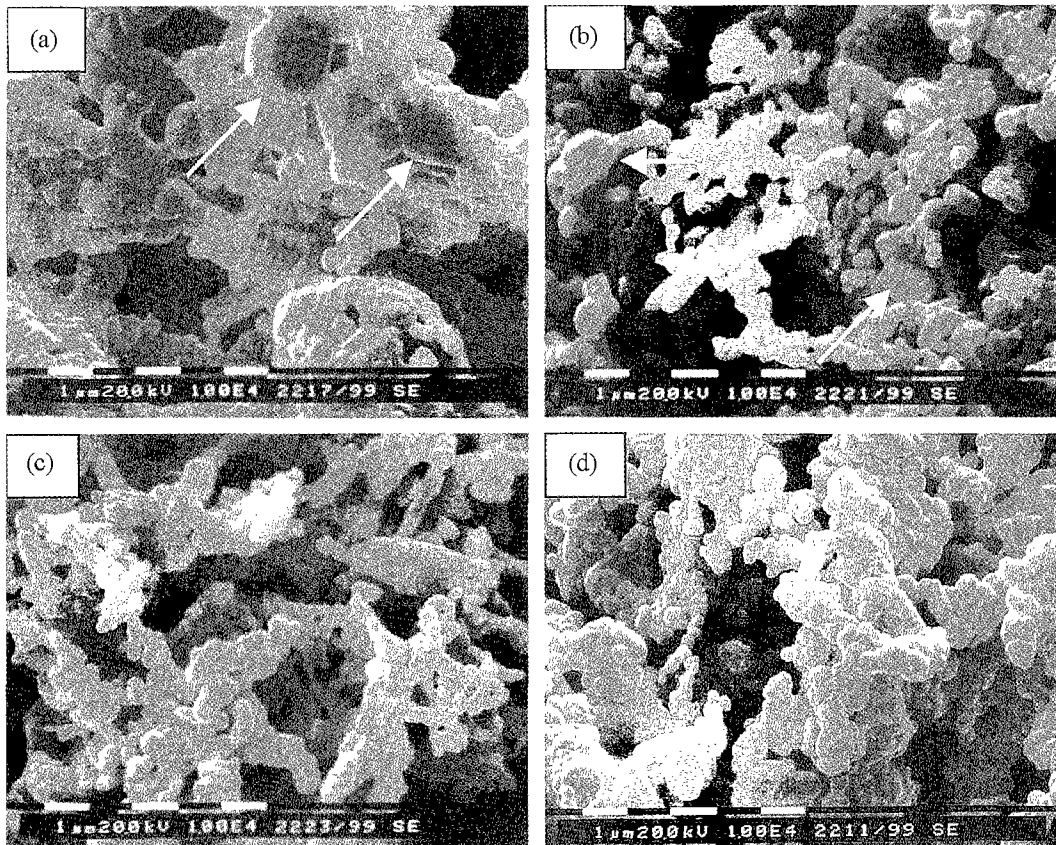


Fig. 9. Scanning electron micrographs of post-heated powder at 800°C for 4 h from (a) R0, (b) R1, (c) R2 and (d) R4 sample.

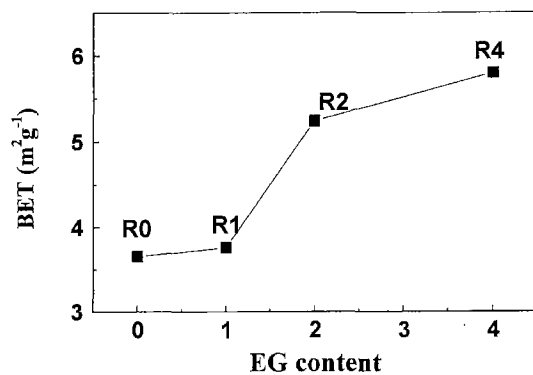


Fig. 10. Dependence of specific surface area of the  $\text{LiMn}_2\text{O}_4$  powder post-heat treated at 800°C 4 hr upon EG content.

tice parameter of  $\text{LiMn}_2\text{O}_4$  is increased with increasing temperature (Fig. 11 (a)). This result is consistent with previous reports.<sup>1,6,16</sup> With increasing the heating temperature, nonstoichiometric oxygen-rich phase ( $\text{Li}_2\text{Mn}_4\text{O}_6$ ) decomposed to  $\text{LiMn}_2\text{O}_4$ , therefore,  $\text{Mn}^{4+}$  (Ionic Radii; 0.530Å) concentration is decreased, while  $\text{Mn}^{3+}$  (Ionic Radii; 0.645Å) increased. Consequently, the lattice parameter of  $\text{LiMn}_2\text{O}_4$  increased.

The lattice parameter of  $\text{LiMn}_2\text{O}_4$  is slowly increased with increasing the amounts of chelate polymers (Fig. 11 (b)).

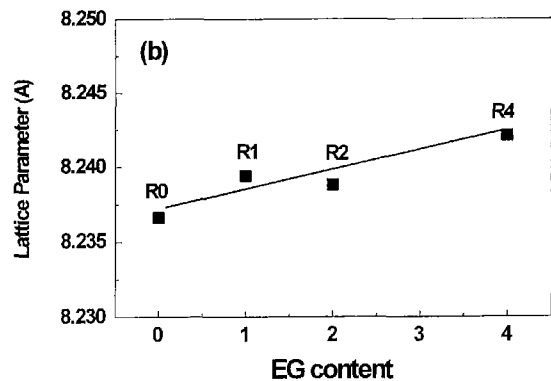
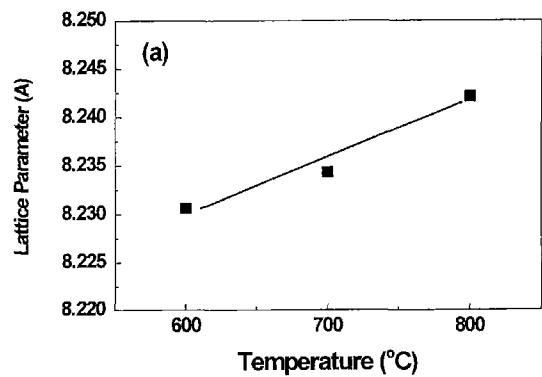


Fig. 11. Dependence of lattice parameter of  $\text{LiMn}_2\text{O}_4$  powder upon (a) postheating temperature and (b) EG content.

This is also consistent with Sun's reports 1). The electrochemical behaviour of this powder for rechargeable Li/ $\text{LiMn}_2\text{O}_4$  cells is reported in other papers.<sup>17,18)</sup>

#### 4. Conclusions

In citrate combustion process, vacuum drying promote the auto-ignition at room temperature. With low addition of EG metal ion was selectively segregated with organic substances and undesired lithium evaporation was occurred during post-heating.  $\text{LiMn}_2\text{O}_4$  phase which is produced by combustion reaction was re-decomposed to  $\text{Mn}_3\text{O}_4$  because the reaction temperature was higher than 950 °C. With increasing EG content, the homogeneity of  $\text{LiMn}_2\text{O}_4$  powder increased and particle size decreased. And lithium evaporation during vacuum drying and/or ignition also increased.

#### Acknowledgement

This work was partly supported by the Brain Korea 21 Project

#### REFERENCES

1. Y-K. Sun, "Synthesis and Electrochemical Studies of spinel  $\text{Li}_{1.03}\text{Mn}_2\text{O}_4$  Cathode Materials Prepared by a Sol-gel Method for Lithium Secondary Batteries," *Solid State Ionics*, **100**, 115-127 (1997).
2. W. Liu, G. C. Farrington, F. Chaput and B. Cunn, "Synthesis and Electrochemical Studies of Spinel Phase  $\text{LiMn}_2\text{O}_4$  Cathode Materials Prepared by the Pechini Process," *J. Electrochem. Soc.*, **143**, 879-884 (1996).
3. Y-K. Choi and B-H. Kim, "Synthesis of  $\text{LiMn}_2\text{O}_4$  Cathode Materials By Emulsion Drying method and Its Electrochemical Properties," *Kor. J. Ceram.*, **5**, 250-254 (1999).
4. S-T. Myung and H-T. Chung, "Preparation and Characterization of  $\text{LiMn}_2\text{O}_4$  Powders by Emulsion Drying Method," *J. Power Sources*, **84**, 32-38 (1999).
5. B. W. Lee and S. H. Kim, "Wet Chemical Preparation of Lithium  $\text{LiMn}_2\text{O}_4$  Spinel By Oxalate Precipitation," *J. Kor. Ceram. Soc.*, **36**, 698-704 (1999).
6. D. H. Jang and S. M. Oh, "Electrolyte Effects on Spinel Dissolution and Cathodic Capacity Losses in 4 V  $\text{Li}/\text{Li}_x\text{Mn}_2\text{O}_4$  Rechargeable Cells," *J. Electrochem. Soc.*, **144**, 3342-3357 (1997).
7. L. W. Tai and P. A. Lessing, "Modified Resin-intermediate Processing of Perovskite Powders : Part I. Optimization of Polymeric Precursors," *J. Mater. Res.*, **7**, 502-515 (1992).
8. Y-S. Han, Y-H. Han, W-S. Song, J-M. Yun, S-H. Lee, I-Y. Seo, S-W. Nam, S-A. Hong and H-I. Yoo, "Development of Planar Type Solid Oxide Fuel Cell," *Proceedings of the 13th Korea-Japan Seminar on New Ceramics*, 150-157 (1996).
9. J. D. Kim, J. W. Moon, G. D. Kim and C. E. Kim, "Preparation of  $(\text{La,Sr})\text{MnO}_3$  Powder by Glycine-nitrate Process Using Oxide as Starting Materials," *J. Kor. Ceram. Soc.*, **34**, 1003-1008 (1997).
10. D-S. Kim, C-W. Ahn, K-W. Jang and K. Cho, "Synthesis of Lithium Aluminate Powder by Combustion Process," Research Report, CM-109, KAERI, 1997.
11. M. Sugawara, M. Ohno and K. Matsuki, "Novel Preparation Method of Manganese(II) Manganese(IV) Oxide ( $\text{Mn}_2\text{Mn}_3\text{O}_8$ ,  $\text{Mn}_5\text{O}_9$ ) by Citrate Process," *Chemistry letters*, 1465-1468 (1991).
12. S. R. Jain, K. C. Adiga and V. R. P. Verneker, "A New approach to Thermochemical Calculations of Condensed Fuel-oxidizer Mixtures," *Combustion and Flame*, **40**, 71-79 (1981).
13. S. T. Aruna, M. Muthuraman and K. C. Patil, "Combustion synthesis and properties of strontium substituted lanthanum manganites  $\text{La}_{1-x}\text{Sr}_x\text{MnO}_3$  (0<x<0.3)," *J. Mat. Chem.*, **7**, 2499-2514 (1997).
14. V. Manev, B. Banov, A. Momchilov and A. Nassalevska, " $\text{LiMn}_2\text{O}_4$  for 4 V lithium-ion batteries," *J. Power Sources*, **57**, 99-112 (1995).
15. A. Momchilov, V. Manev and A. Nassalevska, "Rechargeable Lithium Battery with Spinel-related  $\text{MnO}_2$  Optimization of the  $\text{LiMn}_2\text{O}_4$  Synthesis Conditions," *J. Power Sources*, **41**, 305-314 (1993).
16. Y. Xia and M. Yoshio, "Studies on Li-Mn-O Spinel System (obtained from melt-impregnation method) as a Cathode for 4 V Lithium Batteries Part II. Optimum spinel from  $\gamma$   $\text{MnOOH}$ ," *J. Power Sources*, **57**, 125-135 (1995).
17. Y-S. Han and H-G. Kim, "Synthesis of  $\text{LiMn}_2\text{O}_4$  with Modified Pechini Method and Characterization as a Cathode for Rechargeable  $\text{Li}/\text{LiMn}_2\text{O}_4$  Cells," *J. Power Sources*, **88**, 161-168 (2000).
18. Y-S. Han, J-T. Son and H-G. Kim, "Characterization of  $\text{LiCu}_x\text{Mn}_{2-x}\text{O}_4$  Spinel, Synthesized by Modified Citrate Process, for Li-ion battery," *Abstr. Autumn Meet. Kor. Electrochem. Soc. Seoul Kor.* 1-2 Oct., Ab. P29 (1999).